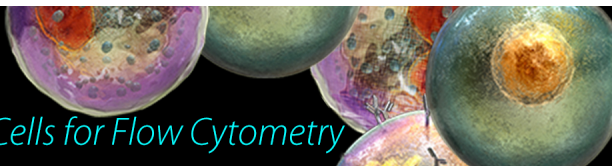


Veri-Cells™

Verified Lyophilized Control Cells for Flow Cytometry



Ion Channels Modulating Mouse Dendritic Cell Functions

Nicole Matzner, Irina M. Zemtsova, Nguyen Thi Xuan, Michael Duszenko, Ekaterina Shumilina and Florian Lang

This information is current as of July 19, 2018.

J Immunol 2008; 181:6803-6809; ;
doi: 10.4049/jimmunol.181.10.6803
<http://www.jimmunol.org/content/181/10/6803>

References This article **cites 31 articles**, 13 of which you can access for free at:
<http://www.jimmunol.org/content/181/10/6803.full#ref-list-1>

Why *The JI*? Submit online.

- **Rapid Reviews! 30 days*** from submission to initial decision
- **No Triage!** Every submission reviewed by practicing scientists
- **Fast Publication!** 4 weeks from acceptance to publication

**average*

Subscription Information about subscribing to *The Journal of Immunology* is online at:
<http://jimmunol.org/subscription>

Permissions Submit copyright permission requests at:
<http://www.aai.org/About/Publications/JI/copyright.html>

Email Alerts Receive free email-alerts when new articles cite this article. Sign up at:
<http://jimmunol.org/alerts>



Ion Channels Modulating Mouse Dendritic Cell Functions¹

Nicole Matzner,* Irina M. Zemtsova,* Nguyen Thi Xuan,* Michael Duszenko,[†]
Ekaterina Shumilina,^{2,3*} and Florian Lang^{2*}

Ca^{2+} -mediated signal transduction pathways play a central regulatory role in dendritic cell (DC) responses to diverse Ags. However, the mechanisms leading to increased $[\text{Ca}^{2+}]_i$ upon DC activation remained ill-defined. In the present study, LPS treatment (100 ng/ml) of mouse DCs resulted in a rapid increase in $[\text{Ca}^{2+}]_i$, which was due to Ca^{2+} release from intracellular stores and influx of extracellular Ca^{2+} across the cell membrane. In whole-cell voltage-clamp experiments, LPS-induced currents exhibited properties similar to the currents through the Ca^{2+} release-activated Ca^{2+} channels (CRAC). These currents were highly selective for Ca^{2+} , exhibited a prominent inward rectification of the current-voltage relationship, and showed an anomalous mole fraction and a fast Ca^{2+} -dependent inactivation. In addition, the LPS-induced increase of $[\text{Ca}^{2+}]_i$ was sensitive to margatoxin and ICAGEN-4, both inhibitors of voltage-gated K^+ (Kv) channels Kv1.3 and Kv1.5, respectively. MHC class II expression, CCL21-dependent migration, and TNF- α and IL-6 production decreased, whereas phagocytic capacity increased in LPS-stimulated DCs in the presence of both Kv channel inhibitors as well as the I_{CRAC} inhibitor SKF-96365. Taken together, our results demonstrate that Ca^{2+} influx in LPS-stimulated DCs occurs via Ca^{2+} release-activated Ca^{2+} channels, is sensitive to Kv channel activity, and is in turn critically important for DC maturation and functions. *The Journal of Immunology*, 2008, 181: 6803–6809.

Dendritic cells (DCs)⁴ are essential for initiating and directing Ag-specific T cell responses. Ca^{2+} -mediated signal transduction pathways play a critical regulatory role in DC responses to diverse Ags, including TLR ligands, intact bacteria, and microbial toxins (1). The phospholipase C- Ca^{2+} pathway seems to be involved in the maturation of monocyte-derived DCs induced by different agonists such as LPS, cholera toxin, dibutyryl-cAMP, and PGE_2 as suggested from the effects of intracellular and extracellular Ca^{2+} chelation (2). Furthermore, addition of Ca^{2+} ionophores to immature DCs results in the acquisition of many morphological and functional properties of activated mature DCs (2–4).

Changes in the cytosolic Ca^{2+} concentration $[\text{Ca}^{2+}]_i$ regulate receptor-mediated endocytosis, phagosome-lysosome fusion, and Ag processing. Upon DC stimulation by diverse soluble and particulate Ags, Calmodulin kinase (CamK) II is activated and inhibition of CamK II results in suppression of cytokine production (5). Another Ca^{2+} -dependent kinase, CamK IV, which is also expressed in DCs, plays a key role in the pathway linking TLR-4 to the control of DC life span (6).

In a number of studies, stimulus-induced changes in $[\text{Ca}^{2+}]_i$ have been observed. Thus, stimulation of DCs by lysophosphatidic acid resulted in a rapid increase in $[\text{Ca}^{2+}]_i$, which was not dependent on the presence of extracellular Ca^{2+} (7). Similarly, ligation of DC-SIGN, a C-type lectin in DCs that mediates capture and internalization of viral, bacterial, and fungal pathogens, triggered rapid and transient intracellular Ca^{2+} mobilization (8). However, the mechanisms and the consequences of this $[\text{Ca}^{2+}]_i$ increase remain unclear.

In macrophages and Kupffer cells, LPS treatment causes an increase in $[\text{Ca}^{2+}]_i$ which is related to TNF- α production (9, 10). Kupffer cells contain L-type voltage-dependent Ca^{2+} channels (11) and thus depolarization of the cell membrane is required for the Ca^{2+} influx into these cells. Contrary to Kupffer cells, DCs have been shown to possess Ca^{2+} release-activated Ca^{2+} channels (CRAC) as a main Ca^{2+} entry pathway (12). Accordingly, Ca^{2+} influx is enhanced by membrane hyperpolarization (12).

The present study explores the mechanism of Ca^{2+} entry into DCs. It is shown that similar to macrophages and Kupffer cells, DCs respond to LPS exposure with a transient increase in $[\text{Ca}^{2+}]_i$. We present evidence for the activation of I_{CRAC} and demonstrate the importance of this activation for DC functions.

In addition, DCs were shown to contain voltage-gated K^+ (Kv) channels, belonging to Kv1 channel family, which are up-regulated by LPS stimulation and play a role in cytokine production (13, 14). In the present study, we address the question whether Kv channels can modulate Ca^{2+} entry in DCs by maintaining the electrochemical driving force for Ca^{2+} influx (15) and thus participate in Ca^{2+} -dependent DC functions.

Materials and Methods

Cell culture

DCs were cultured from bone marrow as previously described (16), with slight modifications. In brief, bone marrow cells were flushed out of the cavities from the femur and tibia of 7–11-wk-old female NMRI mice (Charles River Laboratories) with PBS. Cells were then washed twice with RPMI 1640 and seeded out at density of 2×10^6 cells per 60-mm dish. Cells were cultured for 6 days in RPMI 1640 (Life Technologies) containing: 10% FCS, 1% penicillin/streptomycin, 1% glutamine, 1% nonessential

*Department of Physiology, University of Tübingen, Gmelinstr. 5, Tübingen, Germany; and [†]Interfaculty Institute of Biochemistry, University of Tübingen, Hoppe-Seyler-Str. 4, Tübingen, Germany

Received for publication April 16, 2008. Accepted for publication September 9, 2008.

The costs of publication of this article were defrayed in part by the payment of page charges. This article must therefore be hereby marked advertisement in accordance with 18 U.S.C. Section 1734 solely to indicate this fact.

¹ This work was supported by the Deutsche Forschungsgemeinschaft DFG (SFB 766) and The International Graduate School (GRK 1302/1) "The PI3K Pathway in Tumor Growth and Diabetes".

² These authors share last authorship.

³ Address correspondence and reprint requests to Dr. Ekaterina Shumilina, Department of Physiology, University of Tübingen, Gmelinstr. 5, Tübingen, Germany. E-mail address: ekaterina.shumilina@uni-tuebingen.de

⁴ Abbreviations used in this paper: DC, dendritic cell; CamK, Calmodulin kinase; CRAC, Ca^{2+} release-activated Ca^{2+} channel; Kv, voltage-gated K^+ ; MgTx, margatoxin.

Copyright © 2008 by The American Association of Immunologists, Inc. 0022-1767/08/\$2.00

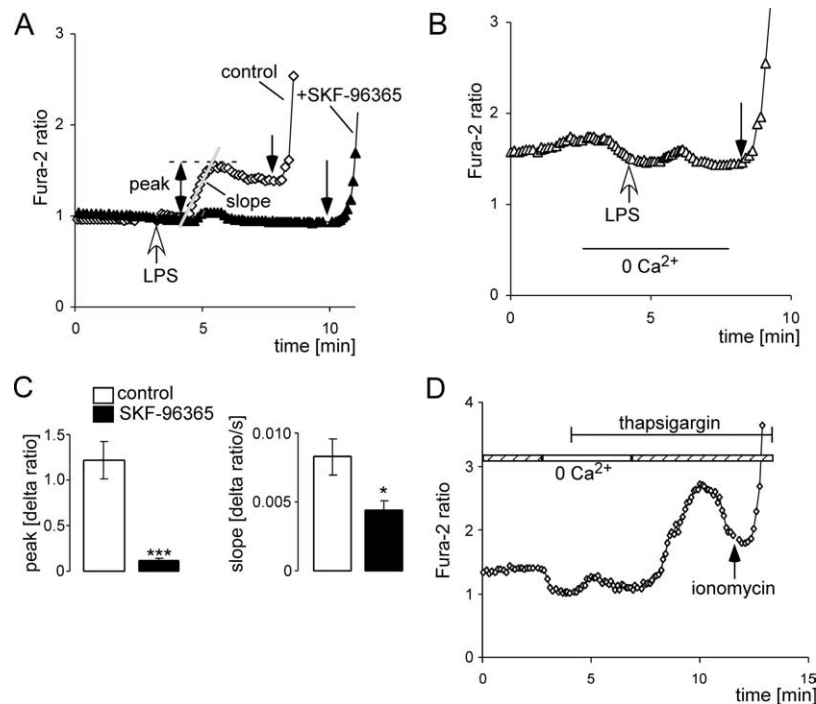


FIGURE 1. LPS exposure increases $[Ca^{2+}]_i$ in DCs. **A**, Representative original tracings showing the fura-2 fluorescence ratios (340/380 nm) in fura-2/AM loaded control and SKF-96365 (10 μ M)-pretreated DCs before and following acute addition of LPS (LPS, 0.1 μ g/ml; white arrow). At the end of each experiment ionomycin (10 μ M; black arrows) was added for calibration purposes. For quantification of Ca^{2+} entry the slope (Δ ratio/s) and peak (Δ ratio) of $[Ca^{2+}]_i$ increase following addition of LPS were calculated. **B**, Representative original tracing showing the fura-2 fluorescence ratio before and following acute addition of LPS in the absence of extracellular Ca^{2+} . To yield a Ca^{2+} -free environment, EGTA (0.5 mM) was added to the Ca^{2+} -free bath solution. **C**, Mean (\pm SEM) of the peak value (left) and slope (right) of the change in fura-2 fluorescence following addition of LPS to the bath solution in the absence ($n = 11$, open bars) and presence ($n = 12$, closed bars) of SKF-96365. *, $p < 0.05$ and ***, $p < 0.001$ indicate significant difference between treated and untreated cells (two-tailed unpaired t test). **D**, Representative tracing showing the fura-2 fluorescence ratio in fura-2/AM loaded DCs. Experiments were conducted before and during exposure to nominally Ca^{2+} -free bath solution. Where indicated, thapsigargin (1 μ M) was added to the nominally Ca^{2+} -free bath solution. Readdition of extracellular Ca^{2+} in the presence of thapsigargin reflects the entry of Ca^{2+} through the store-operated Ca^{2+} entry.

amino acids, and 0.05% 2-ME. Cultures were supplemented with GM-CSF (35 ng/ml, PeproTech) and fed with fresh medium containing GM-CSF on days 3 and 6. Nonadherent and loosely adherent cells were harvested after 6 days of culture. At day 7, >95% of the cells expressed CD11c, which is a marker for mouse DCs. Experiments were performed on mature DCs at days 7–9.

Immunostaining and flow cytometry

Cells (4×10^5) were incubated in 100 μ l FACS buffer (PBS plus 0.1% FCS) containing fluorochrome-conjugated Abs at a concentration of 10 μ g/ml. A total of 2×10^4 cells were analyzed. The following Abs (all from BD Pharmingen) were used for staining: FITC-conjugated anti-mouse CD11c, clone HL3 (Armenian Hamster IgG1, λ 2), PE-conjugated anti-mouse CD86, clone GL1 (Rat IgG2a, κ), PE-conjugated rat anti-mouse I-A/I-E, clone M5/114.15.2 (IgG2b, κ) and PE-conjugated anti-mouse ICAM-1 (CD-54), clone 3E2 (Armenian Hamster IgG1, κ). After incubating with the Abs for 60 min at 4°C, the cells were washed twice and resuspended in FACS buffer for flow cytometry analysis.

Measurement of intracellular Ca^{2+}

Fluorescence measurements were conducted with an inverted phase-contrast microscope (Axiovert 100, Zeiss). Cells were excited alternatively at 340 or 380 nm and the light was deflected by a dichroic mirror into either the objective (Fluar 40 \times 1.30 oil, Zeiss) or a camera (Proxitronic). Emitted fluorescence intensity was recorded at 505 nm and data acquisition was accomplished by using specialized computer software (Metafluor, Universal Imaging). As a measure for the increase of cytosolic Ca^{2+} activity, the slope and peak of the changes in the 340/380 nm ratio were calculated for each experiment.

DCs were pretreated at 37°C with either the I_{CRAC} inhibitor SKF-96365 (10 μ M, 30 min; Sigma-Aldrich), or both margatoxin (MgTx, 1 nM, 30 min; Alomone Laboratories) and ICAGEN-4 (10 μ M, 30 min; Ref. 17), inhibitors of Kv1.3 and Kv1.5, respectively, or left untreated. The cells were loaded with fura-2/AM (2 μ M, Molecular Probes) for 30 min at 37°C.

Intracellular Ca^{2+} was measured before and following addition of LPS from *Escherichia coli* (0.1 μ g/ml; Sigma-Aldrich) in the absence or presence of extracellular Ca^{2+} . When the cells were pretreated with channel inhibitors, the respective inhibitors were added to the bath solutions.

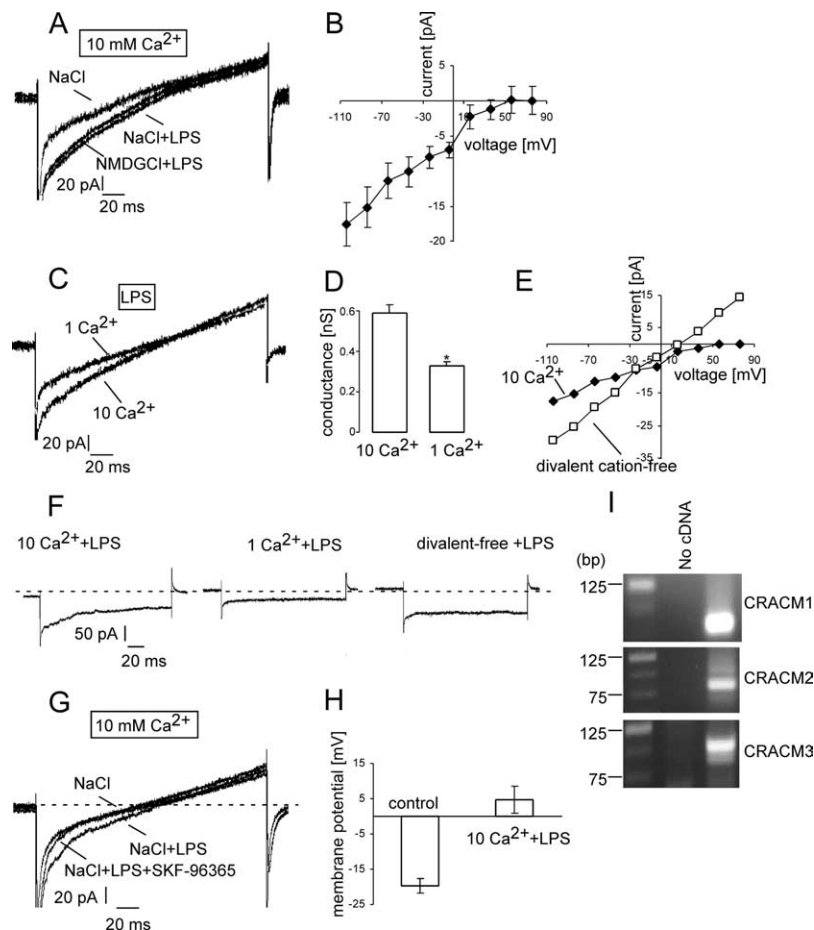
Alternatively, changes in cytosolic Ca^{2+} were monitored upon depletion of the intracellular Ca^{2+} stores. Experiments were conducted before and during exposure to Ca^{2+} -free solution. In the absence of Ca^{2+} the intracellular Ca^{2+} stores were depleted by inhibition of the vesicular Ca^{2+} pump by thapsigargin (1 μ M, Molecular Probes).

Experiments were performed with Ringer solution containing: 125 mM/l NaCl, 5 mM/l KCl, 1.2 mM/l $MgSO_4$, 2 mM/l $CaCl_2$, 2 mM/l Na_2HPO_4 , 32 mM/l HEPES, and 5 mM/l glucose (pH 7.4). Nominally Ca^{2+} -free solutions contained: 125 mM/l NaCl, 5 mM/l KCl, 1.2 mM/l $MgSO_4$, 2 mM/l Na_2HPO_4 , 32 mM/l HEPES, 0.5 mM/l EGTA, and 5 mM/l glucose (pH 7.4). For calibration purposes ionomycin (10 μ M, Sigma-Aldrich) was applied at the end of each experiment.

Patch clamp

Patch clamp experiments were performed at room temperature in voltage-clamp, fast-whole-cell mode according to Hamill et al. (18). The cells were continuously superfused through a flow system inserted into the dish. The bath was grounded via a bridge filled with NaCl Ringer solution. Borosilicate glass pipettes (1–3 MOhm tip resistance; GC 150 TF-10, Clark Medical Instruments) manufactured by a microprocessor-driven DMZ puller (Zeitz) were used in combination with a MS314 electrical micro-manipulator (MW, Märzhäuser). The currents were recorded by an EPC-9 amplifier (Heka) using Pulse software (Heka) and an ITC-16 Interface (Instrutech). For I_{CRAC} measurements whole-cell currents were elicited by 200 ms square wave voltage pulses from -100 to $+80$ mV in 20 mV steps delivered from a holding potential of 0 mV. Alternatively, the currents were recorded with 200 ms voltage ramps from -120 to $+100$ mV. Kv whole-cell currents were elicited by 200 ms square wave voltage pulses from -90 to $+90$ mV in 20 mV steps delivered at 20 ms intervals from

FIGURE 2. Entry of extracellular Ca^{2+} upon LPS-stimulation of DCs is mediated by I_{CRAC} . **A**, Original ramp currents recorded with CsCl/NaCl pipette solution under control conditions (NaCl/10 Ca^{2+}), 2 min after addition of LPS (100 ng/ml) and then upon substitution of Na^+ by NMDG $^+$. **B**, Mean current-voltage (I/V) relationships (\pm SEM, $n = 9$) of current fraction activated by LPS recorded in NaCl/10 mM Ca^{2+} bath solution. **C**, LPS-induced original ramp currents recorded in response to voltage ramps in NaCl bath solution containing either 1 mM Ca^{2+} (and 9 mM Mg^{2+}) or 10 mM Ca^{2+} . **D**, Mean whole-cell conductance of inward currents (\pm SEM, $n = 3$) in NaCl bath solution containing either 10 mM Ca^{2+} or 1 mM Ca^{2+} . Data were calculated by linear regression of I/V curves between -100 and -20 mV. *, $p < 0.05$ indicates significant difference (two-tailed paired t test). **E**, I/V curves of the LPS-activated current fractions obtained in NaCl/10 mM Ca^{2+} -containing or divalent-free bath solutions. **F**, Original current traces at -100 mV obtained upon LPS stimulation in NaCl bath solution containing 10 mM Ca^{2+} (left), 1 mM Ca^{2+} , 9 mM Mg^{2+} (middle), or no divalent cations (right). **G**, Original ramp currents recorded in NaCl bath solution containing 10 mM Ca^{2+} under control conditions (NaCl), 2 min after addition of LPS (100 ng/ml, NaCl plus LPS), and then upon inhibition of the current by SKF-96365 (10 μM , NaCl plus LPS plus SKF-96365). **H**, Mean membrane potential (\pm SEM, $n = 9$) in DCs before (control) and after stimulation with LPS (10 Ca^{2+} + LPS). **I**, Agarose gels with PCR products specific for CRACM1, CRACM2, and CRACM3 channels amplified from cDNA of mouse DCs.



a holding potential of -70 mV. The currents were recorded with an acquisition frequency of 10 and 3 kHz low-pass filtered.

For I_{CRAC} measurements, cells were superfused with a bath solution containing: 140 mM/l NaCl, 5 mM/l KCl, 20 mM/l glucose, 10 mM/l HEPES/NaOH (pH 7.4), and the indicated concentration of divalent cations (0, 1, or 10 mM/l CaCl_2 and 0, 1, or 10 mM/l MgCl_2). A divalent-free bath solution contained 0.5 mM/l EGTA. In some experiments, extracellular Na^+ was substituted by NMDG $^+$ and the bath solution contained: 145 mM/l NMDG-Cl, 10 mM/l HEPES/NMDG, 20 mM/l glucose, 1 mM/l MgCl_2 , and 10 mM/l CaCl_2 . The patch clamp pipettes were filled with an internal solution (CsCl/NaCl pipette solution) containing: 120 mM/l CsCl, 35 mM/l NaCl, 1 mM/l MgATP , 10 mM/l EGTA, and 10 mM/l HEPES/CsOH (pH 7.4).

For Kv current measurements, the cells were superfused with a bath solution containing: 140 mM/l NaCl, 5 mM/l KCl, 1 mM/l MgCl_2 , 2 mM/l CaCl_2 , 20 mM/l glucose, and 10 mM/l HEPES/NaOH (pH 7.4). The patch clamp pipettes were filled with an internal solution (KCl/K-gluconate pipette solution) containing: 80 mM/l KCl, 60 mM/l K^+ -gluconate, 1 mM/l MgCl_2 , 1 mM/l Mg-ATP , 1 mM/l EGTA, 10 mM/l HEPES/KOH (pH 7.2).

Where indicated, SKF-96365 (10 μM , Sigma-Aldrich) or a combination of margatoxin (MgTx, 0.1 nM, Alomone Laboratories) and ICAGEN-4 (10 μM , Ref. 17) was added to the bath solution.

RT-PCR

Total RNA was isolated from mouse DCs by using the Qiashredder and RNeasy Mini Kit from Qiagen. For cDNA first strand synthesis, 1 μg of total RNA in 12.5 μl of DEPC- H_2O was mixed with 1 μl of oligo-dT primer (500 $\mu\text{g}/\text{ml}$, Invitrogen) and heated for 2 min at 70°C . A mix of 2 μl of 10 \times reaction buffer (Biolabs), 1 μl of dNTP mix (dATP, dCTP, dGTP, dTTP, 10 mM each, Promega), 0.5 μl of recombinant RNase inhibitor (Roche), 0.1 μl of M-MuLV reverse transcriptase (Biolabs), and 2.9 μl of DEPC- H_2O was then added and the reaction mixture was incubated for 60 min at 42°C . The reaction was stopped by heating the mixture for 5 min at 94°C . The cDNA was stored at -80°C until PCR analysis. PCR analysis was then performed with 1 μl of the reverse transcription product in a total volume of 25 μl of a PCR mix containing 22 μl of sterile bi-distilled H_2O , 1 μl of sense primer (100 pmol/

μl), 1 μl of antisense primer (100 pmol/ μl), and 1 puReTaq Ready-To-Go PCR bead (Amersham Biosciences) through 40 cycles (30 s at 95°C ; 20 s at 58°C (CRACM1), at 56°C (CRACM2), or at 52°C (CRACM3); 45 s at 72°C). The following primers were used to amplify specific cDNA fragments from mouse DCs: Mouse CRACM1: sense primer: 5'-CATGGTAGCGATGGTGGAAGTC-3'; antisense primer: 5'-TGCTCATCGTCTTTAGTGCCT-3'. Mouse CRACM2: sense primer: 5'-ATGGTGGCCATGGTGGAGGT-3'; antisense primer: 5'-ATTGCCTTCAGCGCTGCA-3'. Mouse CRACM3: sense primer: 5'-AAGCTCAAAGCCTCCAGCCGC-3'; antisense primer: 5'-GGTGGTATTCATGATCGTCT-3'. PCR products were analyzed by agarose gel electrophoresis.

Cytokine measurement

TNF- α and IL-6 concentrations in DC culture supernatants were determined by using OptEIA ELISA kit (BD Pharmingen) according to the manufacturer's protocol.

DC phagocytosis assay

DCs (10^6 cells/ml) were suspended in prewarmed serum-free RPMI 1640 medium, pulsed with FITC-conjugated dextran (Sigma-Aldrich) at a final concentration of 1 mg/ml, and incubated for 3 h at 37°C . Uptake of FITC-conjugated dextran was stopped by adding ice-cold PBS. The cells were then washed three times with ice cold PBS supplemented with 5% FCS and 0.01% sodium azide before FACS analysis.

DC migration assay

DCs were washed twice with PBS and resuspended in RPMI 1640 medium. Migration was assessed in triplicate in a multiwell chamber with 8- μm pore size filter (Calbiochem). The cell suspension (5×10^5 cells/ml) was placed in the upper chamber to migrate into the lower chamber in which either CCL21 (250 ng/ml, PeproTech) or medium alone as a control for spontaneous migration were included. The chamber was placed in a 5% CO_2 37°C incubator for 4 h. The cells that migrated into the lower chamber were detached using Cell Detachment Buffer containing Calcein-AM fluorescent dye. The results were read using a standard fluorescence plate

reader. The mean fluorescence of spontaneously migrated cells was subtracted from the total fluorescence of migrated cells.

Statistics

Data are provided as means \pm SEM, n represents the number of independent experiments. Differences were tested for significance using Student's unpaired and paired two-tailed t test or ANOVA. $p < 0.05$ was considered statistically significant.

Results

Stimulation of DCs with LPS (100 ng/ml) resulted in a rapid increase in $[Ca^{2+}]_i$ (Fig. 1A). This increase was due to Ca^{2+} release from intracellular stores and influx of extracellular Ca^{2+} . Accordingly, removal of extracellular Ca^{2+} (Fig. 1B) or the presence of SKF-96365, a known inhibitor of store-operated channels (10 μ M, Fig. 1, A and C), significantly blunted but did not fully abrogate the increase of $[Ca^{2+}]_i$ following LPS treatment. Store-operated Ca^{2+} entry in mouse DCs could be routinely measured upon store depletion by inhibition of the vesicular Ca^{2+} -ATPase by thapsigargin (Fig. 1D) and thus, we hypothesized that LPS treatment may lead to activation of CRAC channels.

To prove this hypothesis, whole-cell voltage clamp experiments were performed to study the entry of extracellular Ca^{2+} upon LPS stimulation of DCs. Within 1.5–3 min, LPS addition activated an inward current with properties similar to I_{CRAC} (Fig. 2, A and B). With Ca^{2+} as charge carrier (10 mM Ca^{2+} in the bath) the LPS-stimulated current reversed at $> +50$ mV (Fig. 2B), indicating high selectivity for Ca^{2+} . In LPS-stimulated cells neither reversal potential of the current/voltage (I/V) relationship nor current amplitude were altered by replacing extracellular Na^+ by NMDG $^+$ (Fig. 2A). The I/V curve of the LPS-stimulated current fraction revealed a prominent inward rectification at negative voltages. Reducing the concentration of external Ca^{2+} in the continued presence of external Na^+ and Mg^{2+} reduced the inward current (Fig. 2, C, D, and F). One of the distinguishable features of CRAC channels is anomalous mole fraction, describing that when external Ca^{2+} concentration is very low (submicromolar range), large Na^+ currents readily flow through the channels (19). In a Na^+ -containing but divalent cation-free external solution, the LPS-stimulated channel exhibited anomalous mole fraction becoming permeable for Na^+ (Fig. 2, E and F). In the presence of extracellular Ca^{2+} , the inward current of LPS-stimulated cells inactivated fast during hyperpolarizing voltage pulses (Fig. 2F). This inactivation was absent when the cells were recorded in a divalent cation-free solution (Fig. 2F). The current was inhibited by 10 μ M SKF-96365, a blocker of store-operated channels (Fig. 2G).

The membrane potential of DCs was measured using the current-clamp mode of the patch-clamp technique. As shown in Fig. 2H, application of LPS led to membrane depolarization from -19.5 ± 2.5 mV ($n = 8$) to $+1.8 \pm 3.5$ mV ($n = 8$).

Recently, the proteins involved in store-operated Ca^{2+} entry have been identified. These are STIM1, a Ca^{2+} sensor in the endoplasmic reticulum (20–22), and Orai 1 (or CRACM1), a pore subunit of the CRAC channel (23–25). Moreover, there are three mammalian homologous CRAC channel proteins, CRACM1, CRACM2, and CRACM3 (26). To test which CRAC channels are expressed in mouse DCs, DNA fragments specific for the cloned mouse CRACM1, CRACM2, and CRACM3 channels were amplified by RT-PCR. The RT-PCR data demonstrated endogenous expression of all three channels in mouse DCs (Fig. 2I).

DCs are known to express voltage-gated K^+ channels belonging to the Shaker (Kv1) family, presumably Kv1.3 and Kv1.5 (13, 14). Accordingly, margatoxin (MgTx, 0.1 nM) and ICAGEN-4 (10 μ M, Ref. 17), blockers of Kv1.3 and Kv1.5, respectively, inhibited Kv-like currents in DCs (Fig. 3A). The current fraction sensitive to

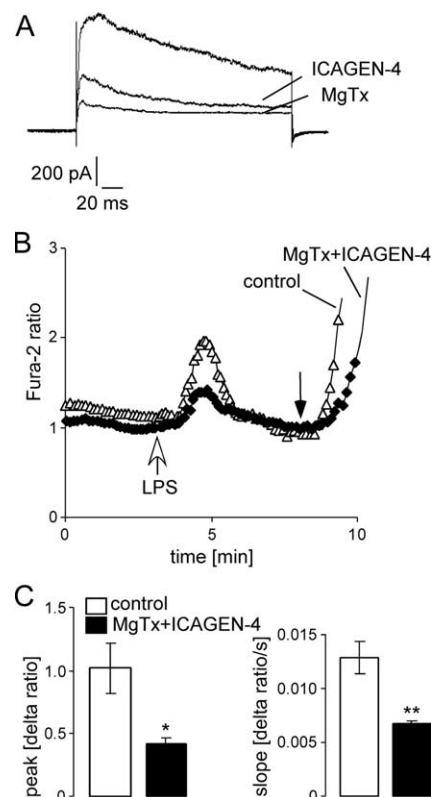


FIGURE 3. Blocking of K_v channels attenuates the increase in $[Ca^{2+}]_i$ upon LPS stimulation of DCs. **A**, Original Kv current traces recorded at $+90$ mV with KCl/K-gluconate pipette solution before and after application of ICAGEN-4 (10 μ M) and then MgTx (0.1 nM). **B**, Representative original tracings showing the fura-2 fluorescence ratios (340/380 nm) in fura-2/AM loaded control and MgTx (1 nM) plus ICAGEN-4 (10 μ M)-pretreated DCs before and following acute addition of LPS. **C**, Mean (\pm SEM) of the peak value (left) and slope (right) of the change in fura-2 fluorescence for control cells ($n = 7$, open bars) and DCs pretreated with MgTx+ICAGEN-4 ($n = 7$, closed bars) following addition of LPS to the bath solution. *, $p < 0.05$ and **, $p < 0.01$ indicate significant difference between both groups (two-tailed unpaired t test).

MgTx (0.1 nM) alone was $54.1 \pm 11.8\%$ ($n = 4$, calculated for the current at $+60$ mV), to ICAGEN-4 (10 μ M) alone $65.7 \pm 3.4\%$ ($n = 8$), and when MgTx (0.1 nM) and ICAGEN-4 (10 μ M) were applied together $84.2 \pm 3.4\%$ ($n = 4$) of the current was inhibited (the amplitude of the remaining current at $+60$ mV was significantly ($p = 0.03$) smaller than under control conditions). To test whether these Kv channels can modulate the Ca^{2+} entry through

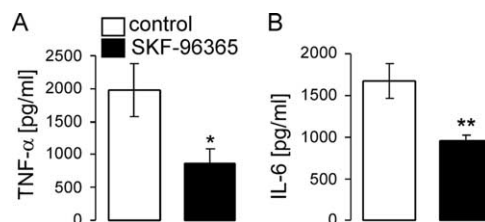


FIGURE 4. SKF-96365 impairs TNF- α and IL-6 production by LPS-stimulated DCs. DCs were incubated with or without 10 μ M SKF-96365 for 30 min before the stimulation with LPS (100 ng/ml). After 4 or 24 h, supernatants were collected to measure TNF- α (A) or IL-6 (B), respectively, by ELISA. The results are representative for three to five independent experiments. Each experiment was performed in duplicates; values represent the mean \pm SEM of duplicates, *, $p < 0.05$ and **, $p < 0.001$, two-tailed unpaired t test.

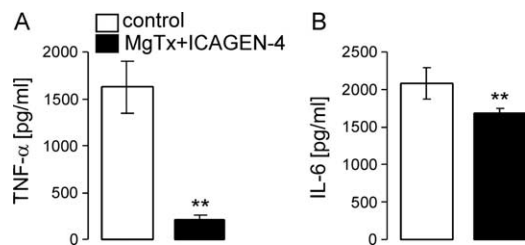


FIGURE 5. Kv channel blockers margatoxin and ICAGEN-4 attenuate TNF- α and IL-6 production by LPS-stimulated DCs. DCs were incubated with or without MgTx (1 nM) plus ICAGEN-4 (10 μ M) for 30 min before the stimulation with LPS (100 ng/ml). After 4 or 24 h, supernatants were collected to measure TNF- α (A) or IL-6 (B), respectively, by ELISA. The results are representative for three to four independent experiments. Each experiment was performed in duplicates; values represent the mean \pm SEM of duplicates, **, $p < 0.01$, two-tailed unpaired t test.

CRAC, the influence of MgTx and ICAGEN-4 on LPS-induced increase in $[Ca^{2+}]_i$ has been determined using fura-2 Ca^{2+} -imaging. As a result MgTx (1 nM) and ICAGEN-4 (10 μ M) significantly reduced the LPS-induced rise in $[Ca^{2+}]_i$ (Fig. 3, B and C).

TNF- α production in LPS-stimulated macrophages has previously been shown to depend on a transient increase in $[Ca^{2+}]_i$ (10). Therefore, we examined the effect of channel blockers on TNF- α production. To this end, DCs were stimulated for 4 h with LPS

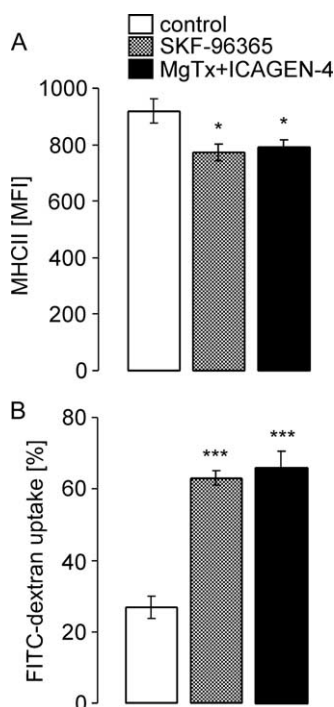


FIGURE 6. SKF-96365 and Kv channel blockers margatoxin and ICAGEN-4 reduce LPS-induced up-regulation of MHC class II and enhance phagocytic capacity of mouse DCs. A, Mean fluorescence intensity (MFI \pm SEM; $n = 5-6$) of MHC class II marker in LPS (100 ng/ml, 48 h)-stimulated DCs incubated in the absence (control, open bar) or in the presence of either SKF-96365 (10 μ M, dotted bar) or MgTx (1 nM) plus ICAGEN-4 (10 μ M) (closed bar). *, ($p < 0.05$) indicate significant difference from control (ANOVA). B, Bar diagram representing mean percent (\pm SEM; $n = 3$) of FITC-dextran uptake by LPS (100 ng/ml, 48 h)-stimulated DCs incubated in the absence (control, open bar) or in the presence of either SKF-96365 (10 μ M, dotted bar), or MgTx (1 nM) plus ICAGEN-4 (10 μ M) (closed bar). ***, $p < 0.001$ indicates significant difference from control (ANOVA).

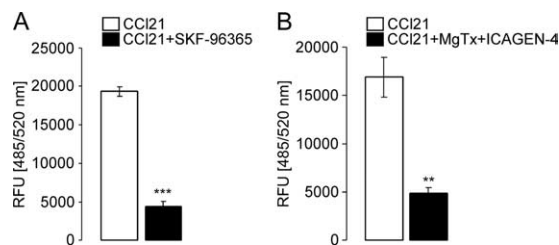


FIGURE 7. SKF-96365 and Kv channel blockers margatoxin and ICAGEN-4 impair CCL21-dependent migration of LPS-stimulated DCs. Mean fluorescence (RFU, relative fluorescence units, \pm SEM; $n = 3-4$) of migrating DCs in response to CCL21. The cells were stimulated by LPS (100 ng/ml, 24 h) either in the absence (open bars, A and B) or in the presence of either SKF-96365 (10 μ M, closed bar, A) or MgTx (1 nM) plus ICAGEN-4 (10 μ M) (closed bar, B). **, $p < 0.01$ and ***, $p < 0.001$, two-tailed unpaired t test.

(100 ng/ml) in the presence or absence of SKF-96365. As a result, treatment with SKF-96365 (10 μ M, 30 min before addition of LPS and then during LPS stimulation) significantly blunted the TNF- α release from LPS stimulated DCs (Fig. 4A). Similarly, MgTx (1 nM) and ICAGEN-4 (10 μ M) significantly reduced the TNF- α release following LPS stimulation (Fig. 5A). Moreover, production of IL-6 was as well significantly reduced by these channel blockers (Figs. 4B and 5B).

Next, we determined whether the maturation and activation of DCs incubated with LPS (100 ng/ml, 48 h) was different in the absence and in the presence of SKF-96365 (10 μ M) or MgTx (1 nM) and ICAGEN-4 (10 μ M). First, cells were collected and stained for MHC class II, CD86, and CD54. The CD11c⁺ gated population was analyzed for the expression of the mentioned markers. There was no significant difference in the expression of CD86 and CD54 before and after activation of LPS in the absence or in the presence of the channel blockers. However, the up-regulation of MHC class II by LPS was significantly reduced by SKF-96365 and MgTx plus ICAGEN-4 (Fig. 6A), indicating that Ca^{2+} entry can be involved in DC maturation.

At the same time, the phagocytic capacity of DCs assessed as FITC-dextran uptake, was dramatically increased by SKF-96365 or MgTx and ICAGEN-4 (Fig. 6B), suggesting that inhibition of CRAC and Kv channels leads to a less mature DC phenotype with higher phagocytic activity.

Ability of DCs to migrate to lymphoid tissues is fundamental for the launching and the coordination of immune responses (27). Therefore, we determined whether DC migration in response to a CCR7 ligand CCL21 is influenced by CRAC and Kv channel blockers. Treatment with SKF-96365 or with MgTx and ICAGEN-4 led to a significant impairment of the ability of LPS-stimulated DCs to migrate in response to CCL21 (Fig. 7).

Discussion

In the present study, we demonstrated that LPS causes a rapid transient increase of cytosolic Ca^{2+} activity ($[Ca^{2+}]_i$) in mouse bone marrow-derived DCs. Removal of extracellular Ca^{2+} or application of SKF-96365, a blocker of store-operated calcium channels (I_{CRAC}) (19), blunted, but did not completely abolish peak and slope of $[Ca^{2+}]_i$ increase. Thus, LPS-induced increase in $[Ca^{2+}]_i$ was partially due to Ca^{2+} influx through Ca^{2+} channels in the plasma membrane and partially due to Ca^{2+} release from intracellular stores. I_{CRAC} has been demonstrated to be the principal Ca^{2+} entry pathway in DCs (12). I_{CRAC} could be activated by store depletion induced by dialyzing the cytosol with inositol 1,4,5-trisphosphate and with high concentration of the Ca^{2+} chelator

BAPTA, which chelates Ca^{2+} that leaks from the stores and hence prevents store refilling (12). Our experiments reveal that LPS strongly activates I_{CRAC} and thus disclose an important mechanism of channel activation.

We further show that the LPS induced $[\text{Ca}^{2+}]_i$ increase in DCs is important for subsequent TNF- α and IL-6 production. Accordingly, inhibition of I_{CRAC} impairs TNF- α and IL-6 secretion. Moreover, LPS-induced up-regulation of MHC class II expression is impaired and phagocytic capacity enhanced in DCs matured in the presence of SKF-96365. In addition, DC migration is dependent on I_{CRAC} activity. Our study thus demonstrates a pivotal role of I_{CRAC} for DC maturation and activity.

I_{CRAC} has been suggested to be important for DC maturation, as activation of I_{CRAC} with thapsigargin induced marked maturation of mouse myeloid DCs (12), human peripheral blood monocytes, and HL-60 cells (3). Also the addition of calcium ionophore to human monocytes or immature DCs resulted in the acquisition of many properties characteristic of activated myeloid DCs (4). However, physiological Ca^{2+} signaling occurs through Ca^{2+} oscillations and not through a long-lasting increase or decrease in $[\text{Ca}^{2+}]_i$ and the activity of signal terminators, such as ER- and plasma membrane-localized Ca^{2+} pumps (SERCA and PMCA, respectively), plasma membrane exchangers (Na^+ - Ca^{2+} exchanger), mitochondrial and cytosolic buffer proteins is extremely important for determination of duration, amplitude, and intracellular location of a particular Ca^{2+} signal (28).

It is important to note that SKF-96365 which is known to inhibit store-operated Ca^{2+} channels, appears to be equally potent in blocking voltage-dependent Ca^{2+} and TRP channels (19) and, thus, cannot be considered as a specific CRAC channel blocker. Recently, the molecules involved in store operated Ca^{2+} entry have been identified. These are STIM1, a Ca^{2+} sensor in the endoplasmic reticulum (20–22), and Orai 1–3 (or CRACM1–3), pore-forming subunits of CRAC channel (23–25). The identification of STIM1 and Orai should allow development of potent and specific inhibitors of CRAC channel in near future.

Entry of positively charged Ca^{2+} through I_{CRAC} is expected to be a function of cell membrane potential and thus K^+ channel activity. Thus, we explored the influence of Kv channels on Ca^{2+} entry. As a result, we indeed observed that Kv channels in DCs sustain the increase of $[\text{Ca}^{2+}]_i$ upon LPS stimulation. They are most probably effective by maintaining the negative membrane potential (29) and providing the necessary electrical driving force for Ca^{2+} influx through I_{CRAC} . Recently, Kv1.3 and Kv1.5 channels were discovered in human blood-derived DCs (13) and bone marrow derived DCs from mice (14). The channels seem to play a role in the maturation process of DCs, because costimulatory molecule expression and cytokine production is decreased in DCs matured in the presence of Kv channel blockers (13, 14). The present study shows that, similar to CRAC blocker SKF-96365, Kv channel blockers led to impaired TNF- α and IL-6 production, decreased LPS-induced up-regulation of MHC II expression, enhanced phagocytic capacity, and reduced migration in mouse DCs and thus provides evidence for novel Kv channel-dependent DC functions. Kv channels are similarly involved in the activation and proliferation of leukocytes (15). Kv1.3 constitutes the dominant K^+ conductance of resting T lymphocytes (30). Inhibition of Kv1.3 channels induces membrane depolarization and prevents the activation response of human T cells (15). Moreover, Kv channels are regulated during proliferation and activation of macrophages (31).

In summary, this study shows that DCs respond to LPS stimulation with a fast increase of $[\text{Ca}^{2+}]_i$, which is accomplished by both, Ca^{2+} release from intracellular stores and Ca^{2+} influx

through I_{CRAC} . The Ca^{2+} influx through I_{CRAC} depends on the activity of Kv channels. Inhibition of either I_{CRAC} or Kv channels leads to profound changes in DC functions, including changes in maturation, phagocytosis, migration, and cytokine production.

Acknowledgments

We gratefully acknowledge the expert technical assistance by Andrea Janessa and the meticulous preparation of the manuscript by Lejla Subasic. We thank Dr. S. Huber and Dr. O. Ureche for helpful discussion.

Disclosures

The authors have no financial conflict of interest.

References

- Connolly, S. F., and D. J. Kusner. 2007. The regulation of dendritic cell function by calcium-signaling and its inhibition by microbial pathogens. *Immunol. Res.* 39: 115–127.
- Bagley, K. C., S. F. Abdelwahab, R. G. Tuskan, and G. K. Lewis. 2004. Calcium signaling through phospholipase C activates dendritic cells to mature and is necessary for the activation and maturation of dendritic cells induced by diverse agonists. *Clin. Diagn. Lab. Immunol.* 11: 77–82.
- Koski, G. K., G. N. Schwartz, D. E. Weng, B. J. Czerniecki, C. Carter, R. E. Gress, and P. A. Cohen. 1999. Calcium mobilization in human myeloid cells results in acquisition of individual dendritic cell-like characteristics through discrete signaling pathways. *J. Immunol.* 163: 82–92.
- Czerniecki, B. J., C. Carter, L. Rivoltini, G. K. Koski, H. I. Kim, D. E. Weng, J. G. Roros, Y. M. Hijazi, S. Xu, S. A. Rosenberg, and P. A. Cohen. 1997. Calcium ionophore-treated peripheral blood monocytes and dendritic cells rapidly display characteristics of activated dendritic cells. *J. Immunol.* 159: 3823–3837.
- Herrmann, T. L., C. T. Morita, K. Lee, and D. J. Kusner. 2005. Calmodulin kinase II regulates the maturation and antigen presentation of human dendritic cells. *J. Leukocyte Biol.* 78: 1397–1407.
- Illario, M., M. L. Giardino-Torchia, U. Sankar, T. J. Ribar, M. Galgani, L. Vitiello, A. M. Masci, F. R. Bertani, E. Ciaglia, D. Astone, et al. 2008. Calmodulin-dependent kinase IV links Toll-like receptor 4 signaling with survival pathway of activated dendritic cells. *Blood* 111: 723–731.
- Panther, E., M. Idzko, S. Corinti, D. Ferrari, Y. Herouy, M. Mockenhaupt, S. Dichmann, P. Gebicke-Haerter, F. Di Virgilio, G. Girolomoni, and J. Norgauer. 2002. The influence of lysophosphatidic acid on the functions of human dendritic cells. *J. Immunol.* 169: 4129–4135.
- Caparros, E., P. Munoz, E. Sierra-Filardi, D. Serrano-Gomez, A. Puig-Kroger, J. L. Rodriguez-Fernandez, M. Mellado, J. Sancho, M. Zubiaur, and A. L. Corbi. 2006. DC-SIGN ligation on dendritic cells results in ERK and PI3K activation and modulates cytokine production. *Blood* 107: 3950–3958.
- Seabra, V., R. F. Stachlewitz, and R. G. Thurman. 1998. Taurine blunts LPS-induced increases in intracellular calcium and TNF- α production by Kupffer cells. *J. Leukocyte Biol.* 64: 615–621.
- Zhou, X., W. Yang, and J. Li. 2006. Ca^{2+} - and protein kinase C-dependent signaling pathway for nuclear factor- κB activation, inducible nitric-oxide synthase expression, and tumor necrosis factor- α production in lipopolysaccharide-stimulated rat peritoneal macrophages. *J. Biol. Chem.* 281: 31337–31347.
- Hijoka, T., R. L. Rosenberg, J. J. Lemasters, and R. G. Thurman. 1992. Kupffer cells contain voltage-dependent calcium channels. *Mol. Pharmacol.* 41: 435–440.
- Hsu, S., P. J. O'Connell, V. A. Klyachko, M. N. Badminton, A. W. Thomson, M. B. Jackson, D. E. Clapham, and G. P. Ahern. 2001. Fundamental Ca^{2+} signaling mechanisms in mouse dendritic cells: CRAC is the major Ca^{2+} entry pathway. *J. Immunol.* 166: 6126–6133.
- Mullen, K. M., M. Rozycka, H. Rus, L. Hu, C. Cudrici, E. Zafranskaia, M. W. Pennington, D. C. Johns, S. I. Judge, and P. A. Calabresi. 2006. Potassium channels Kv1.3 and Kv1.5 are expressed on blood-derived dendritic cells in the central nervous system. *Ann. Neurol.* 60: 118–127.
- Shumilina, E., N. Zahir, N. T. Xuan, and F. Lang. 2007. Phosphoinositide 3-kinase dependent regulation of Kv channels in dendritic cells. *Cell. Physiol. Biochem.* 20: 801–808.
- Cahalan, M. D., H. Wulff, and K. G. Chandy. 2001. Molecular properties and physiological roles of ion channels in the immune system. *J. Clin. Immunol.* 21: 235–252.
- Inaba, K., M. Inaba, N. Romani, H. Aya, M. Deguchi, S. Ikehara, S. Muramatsu, and R. M. Steinman. 1992. Generation of large numbers of dendritic cells from mouse bone marrow cultures supplemented with granulocyte/macrophage colony-stimulating factor. *J. Exp. Med.* 176: 1693–1702.
- Strutz-Seeböhm, N., I. Gutcher, N. Decher, K. Steinmeyer, F. Lang, and G. Seeböhm. 2007. Comparison of potent Kv1.5 potassium channel inhibitors reveals the molecular basis for blocking kinetics and binding mode. *Cell. Physiol. Biochem.* 20: 791–800.
- Hamill, O. P., A. Marty, E. Neher, B. Sakmann, and F. J. Sigworth. 1981. Improved patch-clamp techniques for high-resolution current recording from cells and cell-free membrane patches. *Pflügers Arch.* 391: 85–100.
- Parekh, A. B., and J. W. Putney, Jr. 2005. Store-operated calcium channels. *Physiol. Rev.* 85: 757–810.

20. Roos, J., P. J. DiGregorio, A. V. Yeromin, K. Ohlsen, M. Lioudyno, S. Zhang, O. Safrina, J. A. Kozak, S. L. Wagner, M. D. Cahalan, et al. 2005. STIM1, an essential and conserved component of store-operated Ca^{2+} channel function. *J. Cell Biol.* 169: 435–445.
21. Liou, J., M. L. Kim, W. D. Heo, J. T. Jones, J. W. Myers, J. E. Ferrell, Jr., and T. Meyer. 2005. STIM is a Ca^{2+} sensor essential for Ca^{2+} -store-depletion-triggered Ca^{2+} influx. *Curr. Biol.* 15: 1235–1241.
22. Zhang, S. L., Y. Yu, J. Roos, J. A. Kozak, T. J. Deerinck, M. H. Ellisman, K. A. Stauderman, and M. D. Cahalan. 2005. STIM1 is a Ca^{2+} sensor that activates CRAC channels and migrates from the Ca^{2+} store to the plasma membrane. *Nature* 437: 902–905.
23. Feske, S., Y. Gwack, M. Prakriya, S. Srikanth, S. H. Puppel, B. Tanasa, P. G. Hogan, R. S. Lewis, M. Daly, and A. Rao. 2006. A mutation in Orai1 causes immune deficiency by abrogating CRAC channel function. *Nature* 441: 179–185.
24. Prakriya, M., S. Feske, Y. Gwack, S. Srikanth, A. Rao, and P. G. Hogan. 2006. Orai1 is an essential pore subunit of the CRAC channel. *Nature* 443: 230–233.
25. Vig, M., C. Peinelt, A. Beck, D. L. Koomoa, D. Rabah, M. Koblan-Huberson, S. Kraft, H. Turner, A. Fleig, R. Penner, and J. P. Kinet. 2006. CRACM1 is a plasma membrane protein essential for store-operated Ca^{2+} entry. *Science* 312: 1220–1223.
26. Gwack, Y., S. Srikanth, S. Feske, F. Cruz-Guilloty, M. Oh-hora, D. S. Neems, P. G. Hogan, and A. Rao. 2007. Biochemical and functional characterization of Orai proteins. *J. Biol. Chem.* 282: 16232–16243.
27. Dubsky, P., H. Ueno, B. Piqueras, J. Connolly, J. Banchereau, and A. K. Palucka. 2005. Human dendritic cell subsets for vaccination. *J. Clin. Immunol.* 25: 551–572.
28. Roderick, H. L., and S. J. Cook. 2008. Ca^{2+} signalling checkpoints in cancer: remodelling Ca^{2+} for cancer cell proliferation and survival. *Nat. Rev. Cancer* 8: 361–375.
29. Lewis, R. S., and M. D. Cahalan. 1995. Potassium and calcium channels in lymphocytes. *Annu. Rev. Immunol.* 13: 623–653.
30. Chandy, K. G., H. Wulff, C. Beeton, M. Pennington, G. A. Gutman, and M. D. Cahalan. 2004. K^{+} channels as targets for specific immunomodulation. *Trends Pharmacol. Sci.* 25: 280–289.
31. Vicente, R., A. Escalada, M. Coma, G. Fuster, E. Sanchez-Tillo, C. Lopez-Iglesias, C. Soler, C. Solsona, A. Celada, and A. Felipe. 2003. Differential voltage-dependent K^{+} channel responses during proliferation and activation in macrophages. *J. Biol. Chem.* 278: 46307–46320.